Journal of Alloys and Compounds, 187 (1992) 193–205
JALCOM 302

High J_c Y–Ba–Cu–O thin films prepared by a spray pyrolysis method

E. Ban and Y. Matsuoka
Department of Physics, Meijo University, Tenpaku-ku, Nagoya 468 (Japan)

H. Ogawa
Department of Transport Machine Engineering, Meijo University, Tenpaku-ku, Nagoya 468 (Japan)

K. Kurosawa
Industrial Research Institute, Aichi Prefectural Government, Nishishinwari, Hitotsugi-cho, Kariya 448 (Japan)

(Received March 17, 1992)

Abstract

Y–Ba–Cu–O thin films were prepared on yttria-stabilized zirconia (YSZ) (100), MgO (100) and $SrTiO_3$ (100) substrates by a spray pyrolysis method. The films on YSZ, which were heated rapidly at 1020–1030 °C and then exposed to argon gas until the furnace cooled to 960–970 °C, showed high J_c values of about 10^4 A cm^{-2} (77 K; 0 T). The films have an aligned grain structure consisting of large plate-like grains over a wide area. The melt-processing method in an argon ambient was found to be useful for the enhancement of the J_c of thin films.

1. Introduction

In order to prepare thin and thick films of superconducting $YBa_2Cu_3O_{7-x}$ (the 1:2:3 compound), a number of fabrication techniques have been used. Among these methods, the non-vacuum techniques such as screen printing [1], spin coating [2] and chemical spray pyrolysis [3] are relatively simple and inexpensive. In particular, the spray pyrolysis method is suitable for preparing thin films at a high deposition rate on both small and large areas with stoichiometry. Almost all films prepared by this method, however, show surface roughness and porous microstructure; so the critical current density J_c is not very high (about 100 A cm^{-2}). This has been attributed to the use of conventional solid-phase sintering methods [3–10], *i.e.* the films have been fired for a relatively long time at a low temperature (800–950 °C at most) in either an air or an oxygen atmosphere. To overcome the difficulty of low J_c, it is desirable to melt the Y–Ba–Cu–O ceramics to reduce the granular and porous structure [11]. In such a case, a brief heat treatment would be required to suppress the interface reaction between the film and the substrate. We have applied the melt-processing method to thin films by

0925-8388/92/$5.00

using a rapid and brief heat treatment and obtained a high J_c value of 4800 A cm^{-2} (77 K; 0 T) as reported in another paper [12]. However, the optimized firing conditions had not been established at that experimental stage. Here we report the effects of the firing conditions on the J_c value of the thin films systematically.

2. Experimental procedure

The Y–Ba–Cu–O films were prepared in a fashion similar to those in the previous study [12]. In ref. 12, we used helium as the ambient gas. It has become evident that there is no great difference between helium and argon for the improvement of J_c. We therefore used argon in this experiment.

To prepare an aqueous solution, $Y(NO_3)_3 \cdot 6H_2O$, $Ba(NO_3)_2$ and $Cu(NO_3)_2 \cdot 3H_2O$ were dissolved in ultrapure water separately and then the solution was mixed in a [Y]:[Ba]:[Cu] = 1:2:3 molar ratio. At the same time, ethanol was added up to 20% to the solution. The YSZ (100), MgO (100) and $SrTiO_3$ (100) used as substrates (3 mm × 10 mm) were chemically etched to a mirror finish. During spray deposition, the substrate was kept at 300 °C on the hot-plate. The temperature of the substrate is monitored continuously during spray deposition with a chromel–alumel thermocouple and is controlled to within ±10 °C. The films spray deposited were pre-heated at 500 °C for 30 min in air. The films thus prepared were fired by a simple rapid heating as follows. Films were directly introduced, within 1 min, into the centre of the tube furnace under flowing argon, which was pre-heated to the desired firing temperature $T_s = 1020$ or 1030 °C. After the films had been fired at T_s for 2 min, the furnace was cooled gradually. When the furnace temperature had fallen to T_h, the gas flow was changed from argon to oxygen, which is the main point in which the work in ref. 12 is different. In ref. 12, the rare gas flow was carried out only when the temperature was T_s. After this, the films were gradually cooled in the furnace with an anneal at 600 °C for 2 h, to room temperature. The flow rates of argon and oxygen were 1 l min^{-1} and 0.5 l min^{-1} respectively.

The thicknesses of the fired films were found to be about 2 μm, using a surface profile meter. The critical temperature T_c and critical current I_c of these films were measured with a standard d.c. four-probe method. The J_c value was calculated by dividing I_c, which was measured at 77 K in a zero magnetic field, by the average cross-sectional area of the film. The J_c value therefore represents the approximate average critical density.

The microstructure of the films was investigated by scanning electron microscopy (SEM), X-ray diffraction (XRD), energy-dispersive X-ray analysis (EDXA) and electron probe microanalysis (EPMA).

3. Experimental results and discussion

We first studied the effects of varying the switching temperature T_h on the J_c value of films formed on YSZ substrates. Figure 1 shows the J_c variation

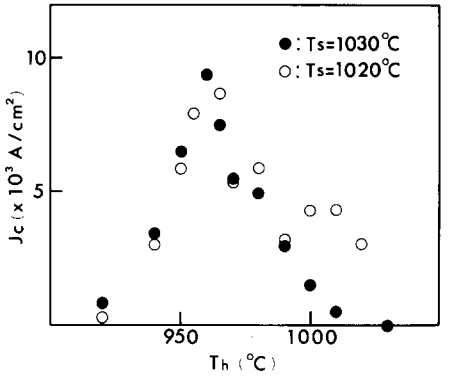

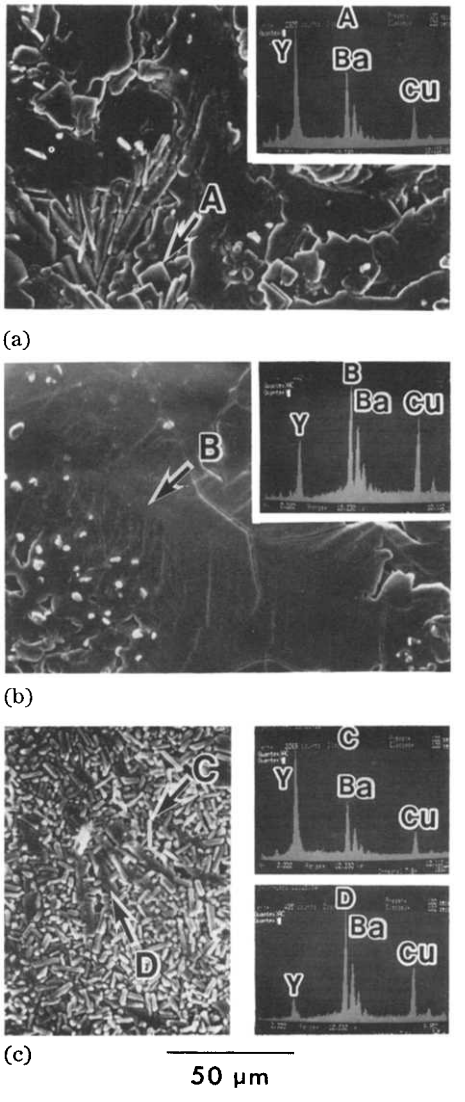

Fig. 1. Critical current density J_c (77 K; 0 T) of films formed on YSZ as a function of the switching temperature T_h at which the flowing gas is changed from argon to oxygen for furnace temperatures T_s of 1030 °C (●) and 1020 °C (○).

Fig. 2. Surface SEM photographs of the film fired at $T_s = 1020$ °C for switching temperatures T_h of (a) 1010 °C, (b) 970 °C and (c) 920 °C. The inset of each photograph shows the EDXA for the region marked by an arrow.

with T_h for the films fired at a constant temperature T_s of 1020 or 1030 °C. The J_c value of both series is found to be very sensitive to T_h. When the films were fired at $T_s = 1040$ °C and above, all films showed poor superconducting properties (300 A cm^{-2} at most) and insulating properties, respectively. On the contrary, J_c for the films fired at $T_s = 1010$ °C or lower

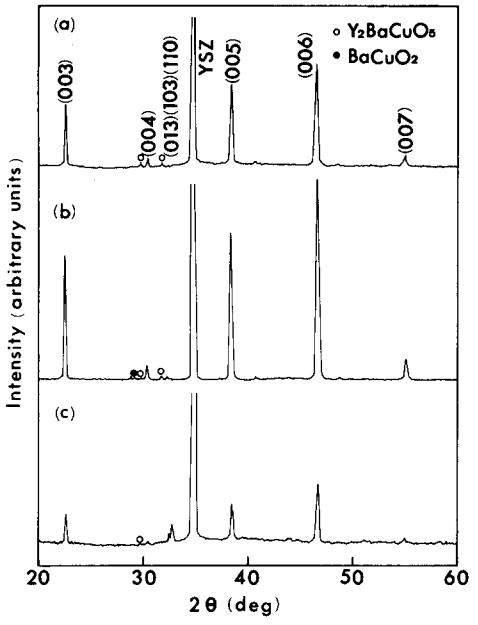

Fig. 3. XRD patterns for the samples shown in Fig. 2.

was 3000–5000 A cm^{-2} at most and decreased abruptly with decreasing T_h. Further enhancement of J_c could not be expected in this low temperature range for the following reasons: (i) the period of heat treatment above the solidus temperature is so short that the periodic reaction of Y_2BaCuO_5 (the 2:1:1 phase) with the liquid phase does not proceed sufficiently and (ii) as mentioned later the crystal growth of Y–Ba–Cu–O itself is prevented because of the deficiency of oxygen in this range.

For convenience, we shall try to classify the data shown in Fig. 1 into three temperature ranges T_h; above 990 °C, 950–980 °C and below 940 °C. Figure 2 shows SEM photographs of three kinds of sample fired at a constant temperature $T_s = 1020$ °C, followed by switching at $T_h = 1010$ °C, 970 °C and 920 °C, respectively, which are the representative temperatures in each region. The inset of each photograph gives the EDXA on the region marked by an arrow. Figure 3 represents the XRD patterns of the same samples as in Fig. 2.

3.1. Temperature region I, $T_h > 990$ °C

The J_c values of films fired at $T_s = 1020$ °C and 1030 °C are 2500–3500 A cm^{-2} and 0–2500 A cm^{-2} respectively. For 1020 °C films, (i) very large grains having a plate- and needle-like structure are observed (Fig. 2(a)), (ii) the oblong-shaped grain (region A) was identified as Y_2BaCuO_5 (the 2:1:1 phase) and (iii) the predominant phase is 1:2:3 with a fairly strong intensity of (00l) reflections, indicating that the preferred orientation of the *c* axis is promoted (Fig. 3(a)). For $T_s = 1030$ °C films, (i) the grain size was smaller than that of 1020 °C films, (ii) XRD patterns showed the reflection peaks

of the 1:2:3 phase with a smaller degree of preferred orientation and the reflection peaks of the 2:1:1 phase with increased intensities compared with the corresponding peaks in the 1020 °C films. These facts give rise to the difference between the J_c of the two series.

Although the data points are considerably scattered, the J_c values of both series tend to decrease with increasing T_h, accompanied by a decrease in grain size and the increase in impurity phases such as the 2:1:1 phase and $BaCuO_2$. This result is characteristic of films exposed to oxygen at a high temperature. Chen *et al.* [13] have reported that incongruent melting of Y–Ba–Cu–O occurs at a temperature about 60 °C lower in a reduced oxygen partial pressure than it does in air. We therefore replaced argon by oxygen in this temperature region while the Y–Ba–Cu–O is still partially melted. As mentioned later, the decomposition of the stoichiometric 1:2:3 phase would be activated under oxygen at a high temperature. This may be the reason why the J_c values are low as a whole in this region. The lower J_c of the 1030 °C films is also attributable to the larger amount of impurities, which is observed in the XRD patterns, because of the higher heating.

3.2. Temperature region II, $T_h = 950$–980 °C

The J_c value is at its highest (5000–9500 A cm^{-2}) in this region. Grain growth is enhanced, and a large plate-like structure up to 300 $\mu m \times 300$ μm in size can be seen over a wide area (Fig. 2(b)). In fact, a black lustre visible to the naked eye could be observed in various places on these films. This structure (region B) was identified as the superconducting 1:2:3 phase by EDXA. All the (00l) peaks in the XRD pattern have pronounced intensities (Fig. 3(b)). In this temperature region, no great difference between the J_c of the 1020 °C films and the 1030 °C films is found, *i.e.* in both series the large plate-like grains grow and stoichiometry is maintained without decomposition from the 1:2:3 phase in a low oxygen partial pressure. These results lead to a high J_c of 9500 A cm^{-2}.

3.3. Temperature region III, $T_h < 940$ °C

The surface of the film is rough as a whole and J_c is as low as 3000 A cm^{-2}. As the switching temperature T_h decreases, J_c decreases. When argon is passed continuously until $T_h < 920$ °C, the XRD peaks corresponding to the 1:2:3 phase become smaller, as shown in Fig. 3(c). Discontinuous small grains with oblong shape (C) and a cloud-like structure (D) can be seen (Fig. 2(c)). Regions C and D are identified as the 2:1:1 phase and an yttrium poor phase respectively by EDXA. For the cloud-like structure D, (i) it was always seen when argon was passed continuously until low T_h, (ii) the molar [Y]:[Ba]:[Cu] ratio was about 1:3.5:7.4, which suggests that it consists of $BaCuO_2 + CuO$ in the main, (iii) the number and the size of these features tended to increase with decreasing T_h and (iv) this structure was also observed in the screen-printed thick film formed with a similar firing condition [14]. These results suggest that the crystal growth of Y–Ba–Cu–O itself is prevented because of the deficiency of oxygen.

Figures 1–3 indicate that aligned grain growth is promoted when the argon flow is maintained until the furnace temperature drops to the range 950–980 °C, and large plate-like grains with a strong c axis alignment would lead to a high J_c value of the film.

The maximum J_c value of about 10^4 A cm^{-2} is four to five times larger than that obtained in a thick film fabricated under similar processing conditions [14]. In the thick film, a higher temperature ($T_s \approx 1060$ °C) was required to melt the whole Y–Ba–Cu–O film in a short firing period. This high temperature treatment is accompanied by the following structural defects: (i) the stoichiometric deviation from the 1:2:3 phase occurs in a fairly wide region in the film, (ii) the reaction between the film and the substrate proceeds and (iii) cracks are easily produced in the film as a result of extended volume reduction. In fact, the size of the plate-like grains in the thick film is smaller than that in the thin film as a whole. On the contrary, these defects would be hard to introduce in the present thin film.

We next examine the effect of a flowing mixture of argon and oxygen on the J_c value of the film. Figure 4 shows variations in the J_c value of the films formed on YSZ *vs.* the mixture ratio of argon to oxygen. Films were fired at $T_s = 1020$ °C by keeping both the switching temperature T_h and the flow rate of mixed gas constant at 1000 °C and 1 l min^{-1} respectively. The ratio $x/(1-x)$ of argon to oxygen was varied according to $x = 1$, 0.95, 0.85, 0.75, 0.5, 0.25 and 0. All films, except for the film with $x = 0$, attained zero resistivity above 77 K and showed a metallic behaviour from room temperature to T_c (onset). The J_c values of data points lying on the horizontal axis are less than 100 A cm^{-2}. For reference, the temperature dependence of the resistivity for the two films with $x = 1$ and $x = 0.5$ is shown in the inset. The T_c (zero) values of both films are 91 K ($x = 1$) and 88 K ($x = 0.5$). It should be noted that the J_c value drastically decreases with increase in the oxygen content. This phenomenon is more marked than in the case of thick films [14], which suggests that the ambient gas exerts its influence on a thin layer

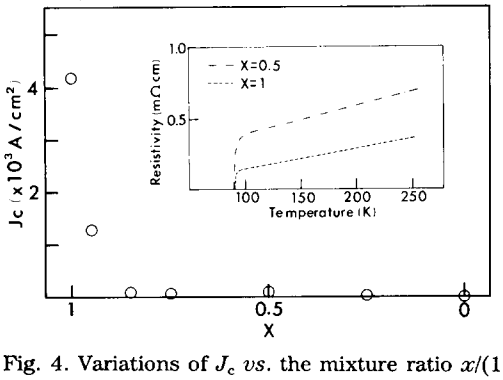

Fig. 4. Variations of J_c *vs.* the mixture ratio $x/(1-x)$ of argon to oxygen. The heat treatment condition is $T_s = 1020$ °C, $T_h = 1000$ °C. The temperature dependence of resistivity for the films with $x = 1$ and $x = 0.5$ are shown in the inset (see text).

(probably a few micrometres) near the surface of the film in our processing conditions.

Figure 5 shows XRD patterns of three samples with $x=1$, $x=0.95$ and $x=0.5$. Some features can be noted on this figure. As the oxygen content increases, (i) the intensity of the (00l) peaks decreases, (ii) the intensity of the impurity peaks corresponding to the 2:1:1 phase and $BaCuO_2$ increases and (iii) the (013), (103) and (110) peaks become stronger and the oxygen-deficient (tetragonal) structure disappears.

Figure 6 shows the surface SEM photographs and the EPMA mapping of yttrium, barium and copper for the same samples as used for Fig. 5. The element profiles were also analysed on the line. As the oxygen content increases, (i) the grain size decreases markedly, (ii) the uniformity in the composition of each element decreases and (iii) copper segregation along grain boundaries becomes pronounced, which causes a deviation from the 1:2:3 phase. It is found from these figures that, when a small amount of oxygen is included in the flowing gas, the plate-like structure with the stoichiometric 1:2:3 phase disappears and granular second phases among the grains increase. These drastic microstructural changes are closely related to the superconducting property J_c, as shown in Fig. 4.

Figures 4–6 indicate that the firing under flowing argon restrains the formation of secondary impurities and promotes the grain growth of the stoichiometric 1:2:3 structure. Mukherjee *et al.* [15] have reported that the oriented grain growth of Y–Ba–Cu–O is improved at low oxygen partial

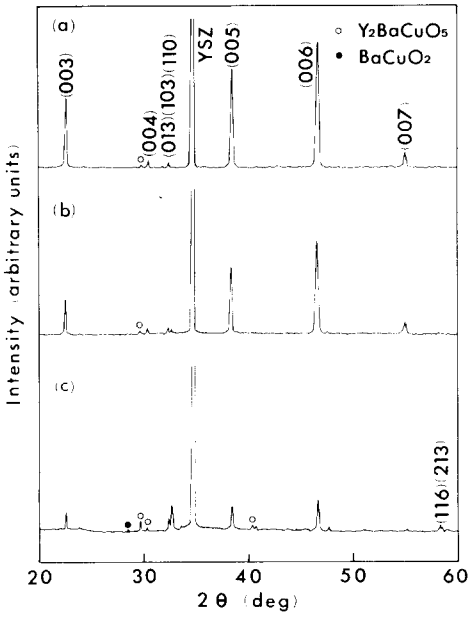

Fig. 5. XRD patterns for the films fired under flowing gas mixture for various argon: oxygen mixture ratios: (a) 1.0:0.0; (b) 0.95:0.05; (c) 0.5:0.5.

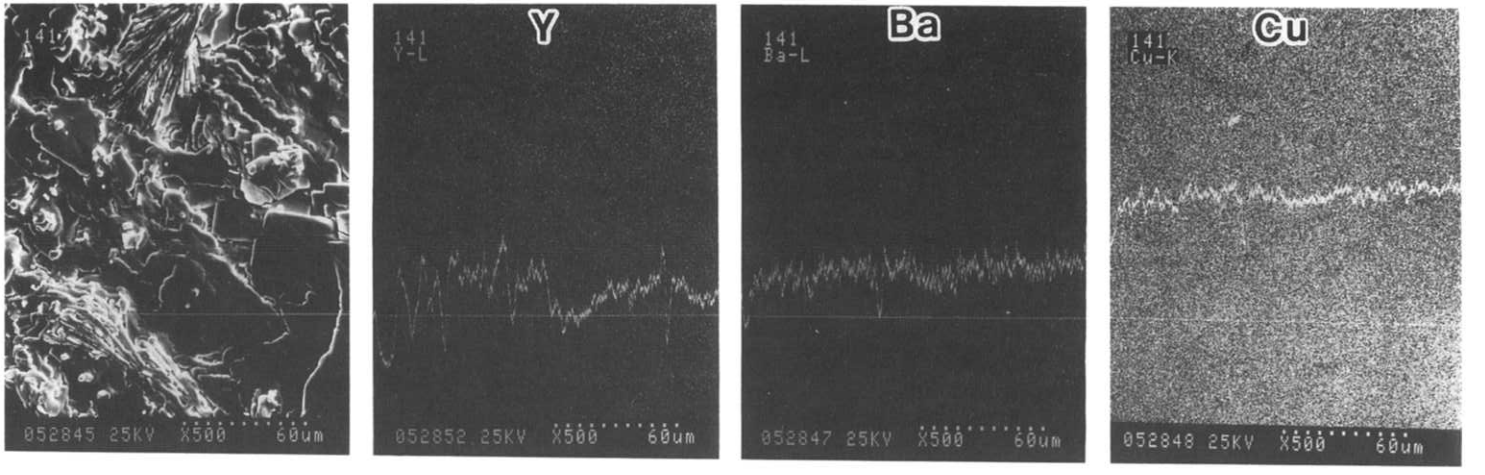

(a)

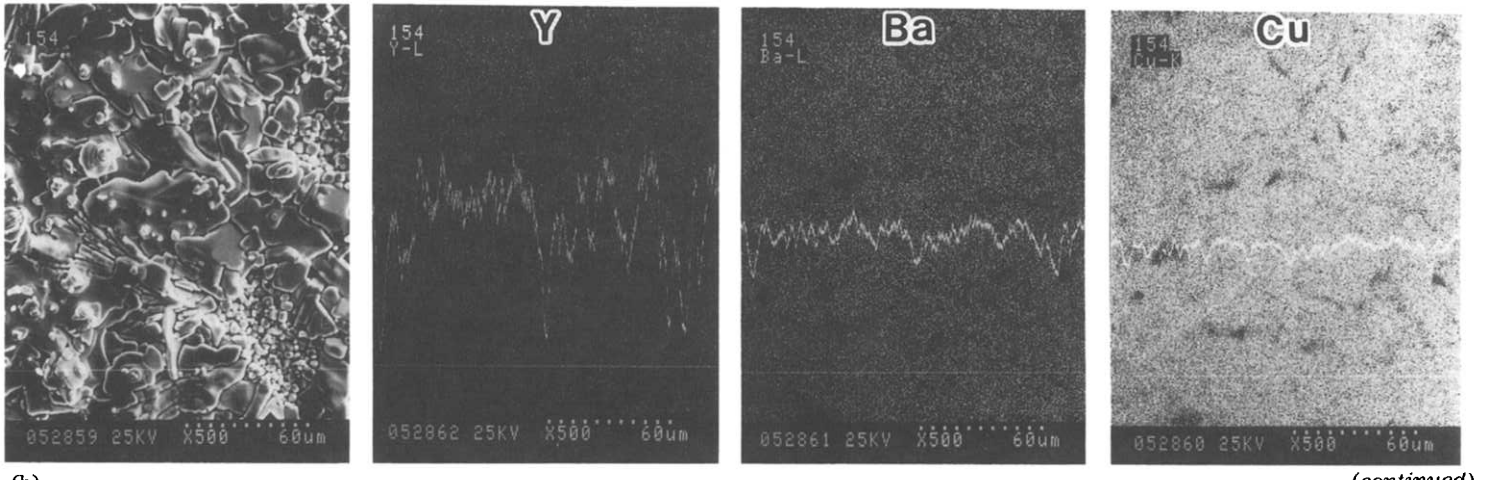

(b)

(continued)

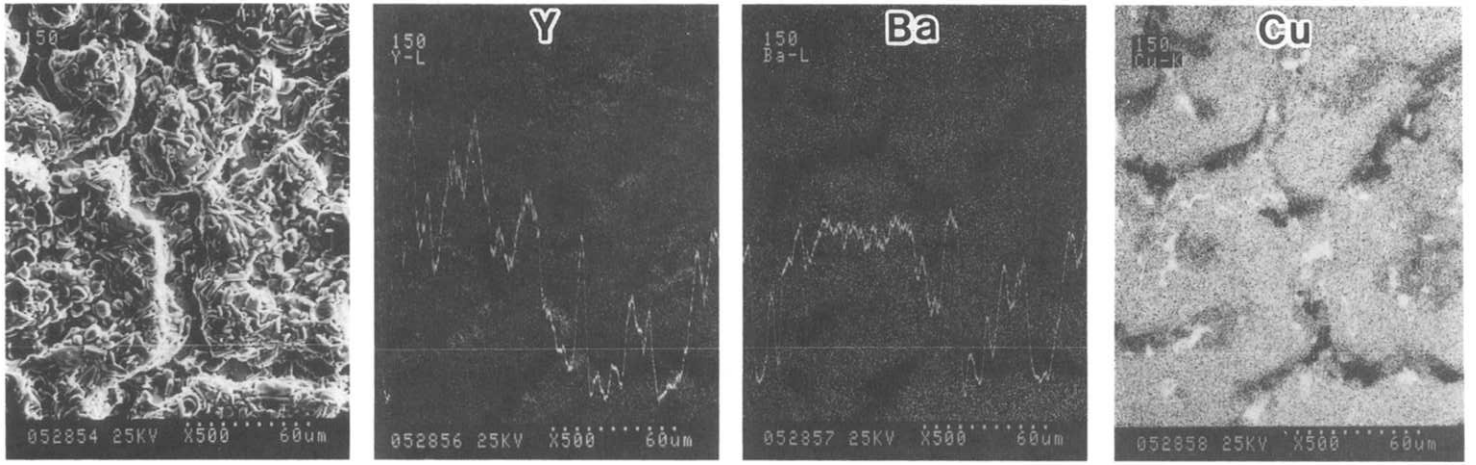

(c)

Fig. 6. Surface SEM photographs and EPMA mapping of yttrium, barium and copper for the films shown in Fig. 5. The element profiles are analysed on the line. The argon:oxygen mixture ratios are (a) 1.0:0.0, (b) 0.95:0.05 and (c) 0.5:0.5.

pressures. Chen *et al.* [13] have also observed that the shrinkage rate and relative density of Y–Ba–Cu–O increase with decrease in the oxygen partial pressure. Manabe *et al.* [16] recently investigated the effect of ambient gas on the reaction between Y–Ba–Cu–O and the YSZ substrate and concluded that the interface reaction decreases in the order air, oxygen and argon. These results qualitatively agree with the present experiment.

In our experiment, the specimen was placed within the furnace tube with its surface parallel to the direction of the gas flow. It was sometimes observed in the same sample that grain growth on the surface exposed upstream differed from that on the surface exposed downstream. Figure 7(a) shows typical surface SEM photographs of the film fired at $T_s = 1020$ °C, $T_h = 970$ °C; on the left is the surface exposed upstream and on the right is the surface exposed downstream. On the upstream side, a large grain of size about 150 μm × 150 μm on the surface is grown. The rectangular structure seen in the centre of the large grain is found to be secondary 2:1:1 phase from EDXA. On the contrary, a parallel needle-like structure and rougher surface can be seen on the downstream side. In the extreme case, discontinuous small particles appeared on the downstream part. The SEM photograph and EPMA mapping shown in Fig. 7(b) is an example of a surface which was fired under similar conditions to the sample in Fig. 7(a). As is found from this figure, the uniformity in composition of each element is lost over a wide region. The detailed mechanism causing this difference is not clear at the present stage. This phenomenon, however, seems to be related to the cooling process [17].

Thin films were prepared on MgO and $SrTiO_3$ substrates fired in the same way as those formed on YSZ. However, these films showed inferior superconducting properties. Figures 8(a) and 8(b) show the XRD patterns and surface SEM photographs of the film ($T_s = 1030$ °C; $T_h = 980$ °C) formed on MgO and $SrTiO_3$ respectively. Large plate-like crystals with preferred c axis orientation were found to be created on the MgO substrate, but its J_c value is very low. The best T_c (zero) and J_c values of the films on MgO were 80 K and 40 A cm^{-2} (77 K; 0 T) respectively. Komatsu *et al.* [18] have reported that the addition of a very small amount of magnesium decreased the J_c. The reason for this degradation has been suggested by Golden *et al.* [19] to be as follows.

(i) Magnesium ions diffuse into the Y–Ba–Cu–O films. The magnesium ions mainly substitute for the copper ions in the Y–Ba–Cu–O lattice because of the similar ionic radii of magnesium and copper. Owing to the difference between the electronegativities of magnesium and copper, the superconductive properties will be greatly affected.

(ii) The stoichiometry is changed because of the diffusion of copper into the substrate. Other researchers [20] have also reported the diffusion of copper into the substrate and the large mobility of copper in the liquid phase of Y–Ba–Cu–O. This interface diffusion is enhanced in our liquid-phase processing and would be the main cause of the poor superconducting properties.

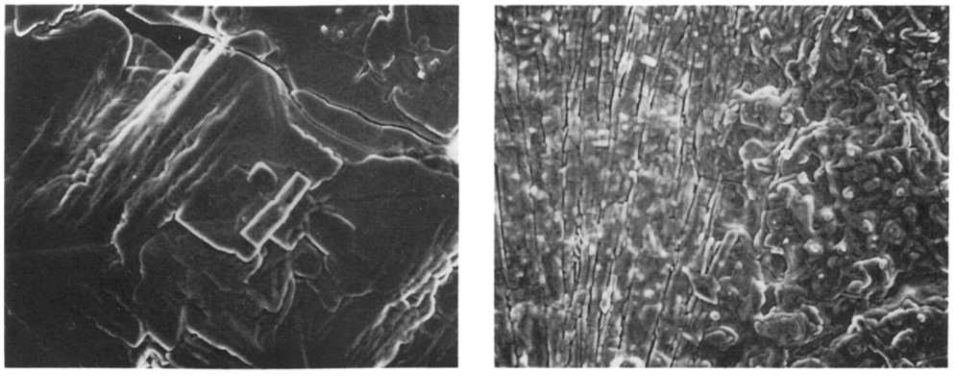

50 μm

(a)

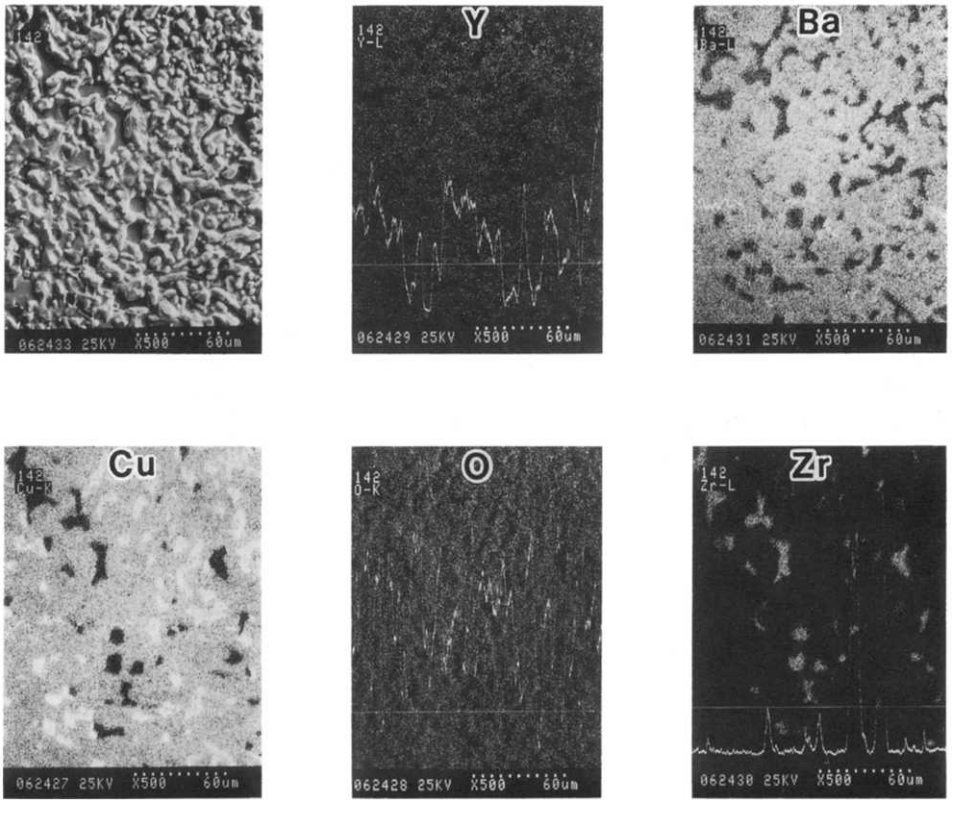

60 μm

(b)

Fig. 7. Surface SEM photographs and EPMA mapping for the films fired at $T_s = 1020$ °C, $T_h = 970$ °C. (a) The upstream side (left) and the downstream side (right) of a typical surface. (b) SEM photograph and EPMA mapping of yttrium, barium, copper, oxygen and zirconium on the downstream part in the extreme case.

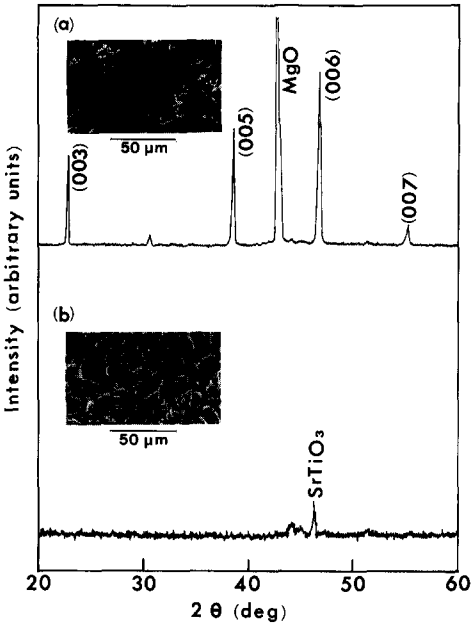

Fig. 8. XRD patterns and surface SEM photographs of the sample fired at $T_s = 1030$ °C, $T_h = 980$ °C, for the substrates (a) MgO and (b) $SrTiO_3$. The intensities in (a) are drawn to a quarter of the scale of those in (b).

On the contrary, the film formed on $SrTiO_3$ did not show any distinct peak of Y–Ba–Cu–O in the XRD pattern except for that of the $SrTiO_3$ substrate. Moreover, SEM observation indicates that the surface of this film looked glassy and its appearance differs considerably from films formed on YSZ and MgO. The room temperature resistivities of all films were extremely high, and no film showed superconductivity above 77 K in our experimental conditions. This may be attributed to contamination of the film due to the diffusion of strontium and/or titanium into the film [21] or to the formation of $YBa_3Ti_2O_{8.5}$ [22].

The most successful substrate in our experiment was YSZ, where $BaZrO_3$ produced by the diffusion of barium ions into the substrate would act as a buffer layer and inhibit further interface reaction [23–25].

4. Conclusions

The main conclusions of this paper are as follows.

(1) Melt-processing in an argon ambient is very useful for the enhancement of J_c values of thin films prepared by the spray pyrolysis method. A maximum J_c of about 10^4 A cm^{-2} is obtained with a firing condition of $T_s = 1020$–1030 °C, $T_h = 960$–970 °C. Large plate-like grains with a strong c axis alignment are observed over a wide area in these films.

(2) The J_c values and the microstructures of the films are very sensitive to the flowing gas. The firing under flowing argon restrains the formation of secondary impurities and promotes the grain growth of stoichiometric 1:2:3 phase.

(3) The most successful substrate is YSZ in our melt-processing method.

Acknowledgments

The authors would like to express their sincere thanks to Y. Hata and O. Mano of Meijo University for their technical assistance. This work was supported by the Hayashi Memorial Foundation for Female Natural Scientists.

References

1 H. Koinuma, T. Hashimoto, T. Nakamura, K. Kishi, K. Kitazawa and K. Fueki, *Jpn. J. Appl. Phys.*, *26* (1987) L761.
2 P. May, D. Jedamzik, W. Boyle and P. Miller, *Supercond. Sci. Technol.*, *1* (1988) 1.
3 M. Kawai, T. Kawai, H. Masuhira and M. Takahashi, *Jpn. J. Appl. Phys.*, *26* (1987) L1740.
4 A. K. Saxena, S. P. S. Arya, B. Das, A. K. Singh, R. S. Tiwari and O. N. Srivastava, *Solid State Commun.*, *66* (1988) 1063.
5 M. Langlet, E. Senet, J. L. Deschanvres, G. Delabouglise, F. Weiss and J. C. Joubert, *J. Less-Common Met.*, *151* (1989) 399.
6 A. Derraa and M. Sayer, *J. Appl. Phys.*, *68* (1990) 1401.
7 R. F. Zhuang, J. B. Qiu and Y. P. Zhu, *J. Solid State Chem.*, *86* (1990) 125.
8 W. J. DeSisto and R. L. Henry, *Appl. Phys. Lett.*, *56* (1990) 2522.
9 S. P. S. Arya and H. E. Hintermann, *Thin Solid Films*, *193–194* (1990) 841.
10 E. Ban, Y. Matsuoka and H. Ogawa, *J. Phys. D*, *22* (1989) 1235.
11 S. Jin, T. H. Tiefel, R. C. Sherwood, M. E. Davis, R. B. van Dover, G. W. Kammlott, R. A. Fastnacht and H. D. Keith, *Appl. Phys. Lett.*, *52* (1988) 2074.
12 E. Ban, Y. Matsuoka and H. Ogawa, *J. Appl. Phys.*, *67* (1990) 4367.
13 N. Chen, D. Shi and K. C. Goretta, *J. Appl. Phys.*, *66* (1989) 2485.
14 Y. Matsuoka, E. Ban, H. Ogawa and A. Suzumura, *Supercond. Sci. Technol.*, *4*(1991) 62.
15 P. S. Mukherjee, A. Simon, P. Guruswamy and A. D. Damodaran, *Solid State Commun.*, *72* (1989) 93.
16 T. Manabe, T. Kumagai, H. Minamiue, S. Nakamura and S. Mizuta, *J. Ceram. Soc. Jpn.*, *98* (1990) 77 (in Japanese).
17 K. Salama, V. Selvamanickam, L. Gao and K. Sun, *Appl. Phys. Lett.*, *54* (1989) 2352.
18 T. Komatsu, H. Meguro, R. Sato, O. Tanaka, K. Matsusita and T. Yamashita, *Jpn. J. Appl. Phys.*, *27* (1988) L2063.
19 S. J. Golden, H. Isotalo, M. Lanham, J. Mayer, F. F. Lange and M. Ruhle, *J. Mater. Res.*, *5* (1990) 1605.
20 T. Teruyama and T. Itoh, *J. Electrochem. Soc.*, *137* (1990) 336.
21 M. H. Frommer, *Supercond. Sci. Technol.*, *3* (1990) 523.
22 W. P. T. Derks, H. A. M. van Hal and C. Langereis, *Physica C*, *156* (1988) 62.
23 M. J. Cima, J. S. Schneider, S. C. Peterson and W. Coblenz, *Appl. Phys. Lett.*, *53* (1989) 710.
24 J. Tabuchi and K. Utsumi, *Appl. Phys. Lett.*, *53* (1988) 606.
25 A. Bailey, G. Alvarez, G. J. Russel and K. N. R. Taylor, *Cryogenics*, *30* (1990) 599.